The need for a new comprehensive view of the middle atmosphere – the potential of infrared limb imaging tomography

Björn-Martin Sinnhuber,[a] Martyn P. Chipperfield,[b] Bianca M. Dinelli,[c] Quentin Errera,[d] Felix Friedl-Vallon,[a] Bernd Funke,[e] Sophie Godin-Beekmann,[f] Alex Hoffmann,[g] Elias Holm,[h] Michael Höpfner,[a] Alizee Malavart,[g] Beatriz M. Monge-Sanz,[i] Marc Op de beeck,[d] Scott Osprey,[i] Enzo Papandrea,[c] Inna Polichtchouk,[h] Peter Preusse,[j] Piera Raspollini,[k] Sebastian Rhode,[j] Martin Riese,[j,l] Pasquale Sellitto,[m,n] Jörn Ungermann,[j] Sarah Vervalcke,[d] Pekka T. Verronen,[o,p] Florian Voet,[j] Kaley A. Walker[q]

[a] *Karlsruhe Institute of Technology, KIT, Karlsruhe, Germany*

[b] *University of Leeds, United Kingdom*

[c] *Institute of Atmospheric Sciences and Climate (CNR-ISAC), Italy*

[d] *Royal Belgian Institute of Space Aeronomy, Belgium*

[e] *Instituto de Astrofísica de Andalucía, CISC, Spain*

[f] *National Centre for Scientific Research, France*

[g] *European Space Agency ESA ESTEC, The Netherlands*

[h] *European Centre for Medium-Range Weather Forecasts, ECMWF*

[i] *University of Oxford, United Kingdom*

[j] *Forschungszentrum Jülich, Jülich, Germany*

[k] *National Research Council, Italy*

[l] *Institute for Atmospheric and Environmental Research, University of Wuppertal, Germany*

[m] *Univ. Paris-Est Créteil and Université de Paris Cité, CNRS, Laboratoire Interuniversitaire des Systèmes Atmosphériques, Institut Pierre Simon Laplace, Créteil, France*

[n] *Istituto Nazionale di Geofisica e Vulcanologia, Osservatorio Etneo, Catania, Italy*

[o] *University of Oulu, Finland*

[p] *Finnish Meteorological Institute, Finland*

[q] *University of Toronto, Canada*

Corresponding author: Björn-Martin Sinnhuber, bjoern-martin.sinnhuber@kit.edu

Early Online Release: This preliminary version has been accepted for publication in *Bulletin of the American Meteorological Society*, may be fully cited, and has been assigned DOI 10.1175/BAMS-D-24-0217.1. The final typeset copyedited article will replace the EOR at the above DOI when it is published.

ABSTRACT

The Earth's middle atmosphere spans the deep region from the upper troposphere/lower stratosphere at around 10 km altitude to the mesosphere/lower thermosphere at around 100 km altitude. It is being increasingly recognized for its role in driving extreme surface weather and regional climate change. Climate models predict large ongoing and future changes in the middle atmosphere composition and circulation. However, the observations needed to detect, attribute and understand these changes and their impacts, to test predictions, and thereby to improve our models, are lacking. Here we show the capacity of infrared limb-imaging tomography to provide the needed observations. This evaluation is based on studies performed within a recent satellite mission concept – the Changing-Atmosphere Infrared Tomography Explorer, CAIRT. Observing thermal infrared emissions simultaneously from the middle troposphere at about 4 km up to the lower thermosphere at about 115 km altitude this technique provides observations of temperature and an extensive range of trace gases with unprecedented spatial resolution of about 50 by 50 km horizontally and about 1 km vertically. We show how these observations would (a) help to quantify the changing atmospheric circulation, (b) allow characterization and quantification of the gravity waves that are critical in driving this circulation, (c) reveal how variability in solar radiation and energetic particles propagate downward to affect regional climate at the surface, (d) detect how volcanic eruptions and wildfires impact the middle atmosphere and climate, and (e) resolve how stratosphere-troposphere exchange affects ozone and water vapor in the crucial and climate-relevant tropopause region.

SIGNIFICANCE STATEMENT

The middle atmosphere serves as a critical link between the Earth's surface, the upper atmosphere, and the near-Earth space environment. It is increasingly influenced by rising greenhouse gas concentrations, ozone layer recovery, biomass burning emissions, and spacecraft activities, pushing the system into uncharted territory. However, current observational capabilities are insufficient to address these emerging challenges, with an imminent "data desert" of middle atmosphere observations. We show with the proposed Changing-Atmosphere Infrared Tomography Explorer, CAIRT, how infrared limb-imaging can provide the urgently needed information on atmospheric waves, circulation patterns, and composition in a changing climate.

Accepted for publication in *Bulletin of the American Meteorological Society.* DOI 10.1175/BAMS-D-24-0217.1.

CAPSULE

Infrared limb imaging from space can provide unique observations of the Earth's middle atmosphere, closing a critical gap in the existing observing system.

Introduction

The deep region between the upper troposphere/lower stratosphere (UTLS) at around 10 km altitude and the mesosphere/lower thermosphere (MLT) at around 100 km altitude is commonly called the middle atmosphere. The middle atmosphere plays a critical role in the climate system by connecting distant geographical regions, linking with the near-earth space environment, and by providing sources of predictability that allow the extension of weather forecasting timescales (e.g., Scaife et al, 2022). An accurate representation of the middle atmosphere and its variability in numerical weather prediction and climate models can lead to better prediction of extreme events and regional climate change, thus reducing the risk on human health, agriculture, infrastructure and water management. Better understanding those processes driving middle atmosphere variability now and in the future is therefore highly important.

The global atmosphere is changing throughout its entire depth from the surface to the fringes of space due to anthropogenic emissions of greenhouse gases, pollutants, aerosol and their precursors, and to the reduction in emissions of ozone-depleting substances (ODSs). This change is occurring against a naturally variable background influenced by, inter alia, volcanic eruptions and solar variability. These changes in composition are closely coupled with changes in circulation, and will affect surface climate, weather (e.g., Kidston et al., 2015) and air quality (e.g., Neu et al., 2014).

While it is now well established that anthropogenic emissions of long-lived greenhouse gases such as CO_2 are the dominant drivers of global climate change (IPCC, 2023), our understanding of decadal climate change at regional scales is still far from complete. Changes in short-lived climate forcers such as stratospheric water vapor (e.g., Solomon et al., 2010), ozone (e.g., Riese et al., 2012; WMO 2022), or stratospheric aerosol (e.g., Solomon et al., 2011; Santer et al., 2014; Ridley et al. 2014) have important impacts on decadal scale and regional climate change. Variability in the stratospheric winter circulation in both hemispheres can influence mid-latitude temperature and precipitation extremes (e.g., King et al., 2019; Lim et al., 2019). Similarly, the quasi-biennial oscillation (QBO), consisting of

Accepted for publication in *Bulletin of the American Meteorological Society.* DOI 10.1175/BAMS-D-24-0217.1.

alternating eastward and westward winds in the tropical stratosphere, can influence tropospheric deep convection and thus extreme precipitation (e.g. Butler et al., 2019).

A large fraction of the Southern Hemisphere (SH) surface climate change in recent decades is attributable to the Antarctic ozone hole and its recovery (Thompson et al., 2011; Oh et al., 2022). Observations indicate a poleward expansion of the tropical Hadley circulation, with possible causes related to greenhouse gas forcing, stratospheric ozone and circulation changes, stratospheric aerosol changes and upper tropospheric pollution (Staten et al., 2018; WMO, 2022, and refs therein).

The large-scale atmospheric circulation plays a central role in connecting the ongoing changes in the middle atmosphere (Figure 1), with the tropics-to-pole Brewer-Dobson circulation (BDC) in the stratosphere and the summer-pole-to-winter-pole circulation in the mesosphere. An acceleration of the BDC is predicted by climate models as a result of increasing greenhouse gases, as well as past stratospheric ozone depletion (e.g., Abalos et al., 2019). A strengthened BDC would have important implications for the transport of trace gases into and throughout the middle atmosphere, affecting processes such as the flux of stratospheric ozone into the troposphere (e.g., Hegglin and Shepherd, 2009; Meul et al., 2018), where it acts as a greenhouse gas, the recovery of the stratospheric ozone layer (Dhomse et al., 2018; Keeble et al., 2021), and the lifetime of ODSs (Butchart and Scaife, 2001; Chipperfield et al., 2014).

Direct measurements of the mean circulation and its changes are not possible due to its slow speed. Instead, the circulation can be examined through its effect on trace constituents using the concept of "age-of-air", the average time an air mass takes to move from near the Earth's surface to a location in the middle atmosphere. This can be determined, for example, through middle atmosphere observations of trace gases that exhibit long-term increasing concentrations at the surface, such as sulfur hexafluoride (SF_6) (e.g., Garny et al., 2024).

A key driver of middle atmosphere circulation and variability is drag from breaking/dissipating waves, including gravity waves. Global observational constraints on gravity wave driving throughout the middle atmosphere are currently lacking, leading to large uncertainties in their representation in climate and weather models (Alexander et al., 2010; Plougonven et al., 2020). These uncertainties affect not only variability in the middle atmosphere but also modelled stratosphere-troposphere dynamical coupling in both hemispheres (Polichtchouk et al., 2018) and thus the predictability of surface extremes.

Accepted for publication in *Bulletin of the American Meteorological Society.* DOI 10.1175/BAMS-D-24-0217.1.

The middle atmosphere critically affects the impact of solar variability on climate. Changes in solar UV radiation, absorbed primarily in the upper and middle atmosphere, are much larger than changes in visible radiation, mostly absorbed at the Earth's surface. Another route for solar impacts on the middle atmosphere is Energetic Particle Precipitation (EPP), either via energetic particles directly produced by the Sun during Solar Proton Events (SPEs) or through Energetic Electron Precipitation (EEP) due to the interaction of the solar wind with Earth's magnetosphere (Sinnhuber and Funke, 2018). EPP enhances ionisation of gases in the polar upper mesosphere and lower thermosphere leading to the formation of nitrogen oxides (collectively called NOy). NOy is transported down to the stratosphere within the winter polar vortex (Funke et al., 2014), affecting ozone layer chemistry, potentially interfering with polar ozone recovery, and ultimately altering dynamics through changes in the radiative balance (Sinnhuber and Funke, 2018; WMO, 2022).

Volcanic eruptions can inject large amounts of sulfur directly into the stratosphere, where the resulting sulfate aerosols affect surface climate through the scattering of solar radiation (e.g., Kremser et al., 2016). In addition to the infrequent large volcanic eruptions, small and medium-sized eruptions lead to a constantly changing background of stratospheric aerosols (Solomon et al., 2011; Stone et al., 2017; Sellitto et al., 2022). Pyroconvection from wildfire biomass burning has in recent years been identified as another contributor to the stratospheric aerosol loading, with the effect of large wildfires being comparable to medium-sized volcanic eruptions (Khaykin et al., 2020).

Because of their efficiency at cooling the planet, artificial enhancement of stratospheric sulfate aerosols has been proposed as a method of solar radiation management ("geoengineering") to counteract climate change (National Academy of Science, 2021; Tilmes et al., 2024). This topic is now regularly assessed as part of the World Meteorological Organisation (WMO)/United Nations Environment Programme (UNEP) Ozone Assessments (e.g. WMO/UNEP 2022 Chapter 6). Such action, should it take place, will require close monitoring and careful understanding of the fate of all stratospheric aerosols and their adverse effects.

A further emerging topic with growing concerns is the impact that the large increase of future space launches and satellite reentry by upcoming mega constellations will have on the middle atmosphere and its composition (e.g., Ferreira et al., 2024; Revell et al., 2025).

Accepted for publication in *Bulletin of the American Meteorological Society.* DOI 10.1175/BAMS-D-24-0217.1.

The scientific challenges outlined above require continued as well as innovative and improved observations of the middle atmosphere. To address these challenges and to provide the urgently needed observations, we proposed the Changing-Atmosphere Infra-Red Tomography Explorer (CAIRT) as a candidate mission for the European Space Agency's planned Earth Explorer 11 satellite. The CAIRT mission concept was thoroughly evaluated during Phase A studies in the competitive mission selection process of ESA's Earth Explorer program. This process culminated in a public review and in an independent scientific assessment by ESA's Advisory Committee for Earth Observation. At the end of the ESA-led Phase A feasibility studies, the CAIRT mission concept was judged to have reached the required scientific readiness and technical maturity for selection and implementation as ESA's Earth Explorer 11. In the competitive mission selection process, the CAIRT mission concept was ranked second and not selected for implementation. In this paper we will give an overview of the CAIRT mission concept and the unique contributions that a future infrared limb-imaging satellite mission can provide to unravel the coupling between composition and circulation in our changing atmosphere.

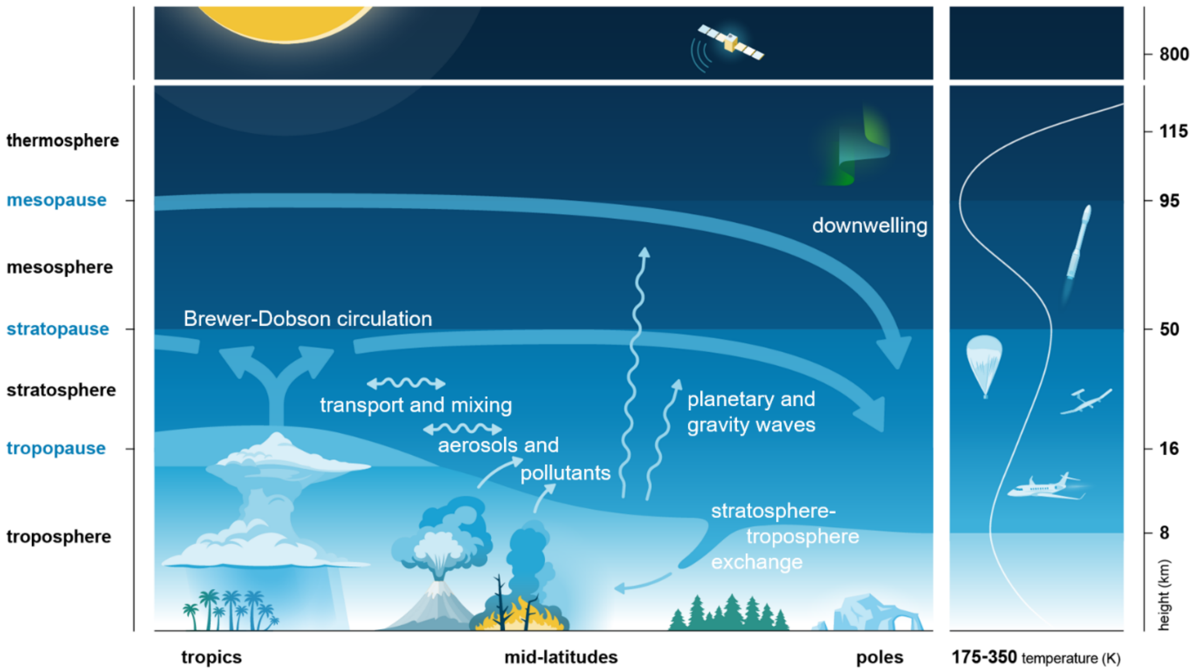

Figure 1. Earth's atmosphere from the surface to the lower thermosphere. Left, schematic overview of the middle atmosphere wave-driven circulation and its intimate connection with atmospheric transport and composition, with the equator-to-pole Brewer-Dobson circulation in the stratosphere and the summer-pole-to-winter-pole circulation in the mesosphere. Right, atmospheric mean temperature profile.

Accepted for publication in *Bulletin of the American Meteorological Society.* DOI 10.1175/BAMS-D-24-0217.1.

The need for observing the changing middle atmosphere: continuity and innovation

Observation, understanding, and attribution of the ongoing changes in the middle atmosphere require measurement of the key constituents and processes involved. Having benefited from more than two decades of intense observations of the middle atmosphere by instruments like the Michelson Interferometer for Passive Atmosphere Sounding (MIPAS) on Envisat (2002-2012), the Microwave Limb Sounder (MLS) on Aura (since 2004), Atmospheric Chemistry Experiment - Fourier Transform Spectrometer (ACE-FTS) on Scisat (since 2003), the Sounding of the Atmosphere using Broadband Emission Radiometry (SABER) being on the Thermosphere Ionosphere Mesosphere Energetics Dynamics (TIMED) satellite (since 2002), and Odin (since 2001), we are facing an imminent "data desert" of middle atmosphere observations (Salawitch et al., 2025). The planned decommissioning of MLS and Odin in the next two years and ACE-FTS and SABER being well beyond their original design lifetime, occur at a particularly critical time. With the ongoing increase in greenhouse gas concentrations and emerging topics of societal concern such as proposed geoengineering by deliberate stratospheric aerosol injection and the atmospheric impact of upcoming satellite mega-constellations we are entering uncharted territory. The need for better understanding and monitoring of climate change in the middle and upper atmosphere is discussed in the perspectives by Plane et al. (2023) and Añel et al. (2025). Chipperfield and Bekki (2023) stress the importance of new satellite limb observations to monitor and study the future development of the stratospheric ozone layer. While the future observing capacity for ozone is reasonably assured (Salawitch et al., 2025), there is in particular a notable lack of future observations of tracers to diagnose changes in atmospheric transport and to attribute observed changes in composition.

In addition to observation continuity, there is a clear need for new innovative observations at higher spatial resolution than available to date. Deviations from the zonal mean by waves, filaments and mixing are essential parts of the middle atmosphere circulation. There is a need to validate the new generation of atmospheric and Earth system models with their increased spatial resolution and to guide future model developments. Various user community requirements (e.g., Global Climate Observing System GCOS-245, 2022) have expressed this need for higher resolution global middle atmosphere temperature and composition measurements with vertical resolution of 1–2 km and horizontal resolution of 100–200 km.

Accepted for publication in *Bulletin of the American Meteorological Society.* DOI 10.1175/BAMS-D-24-0217.1.

Such observations are needed to resolve the sharp tracer gradients across the tropopause, to detect filaments and plumes from wildfires or volcanic eruptions and, very importantly, to resolve atmospheric gravity waves. Gravity waves play a critical role in driving the middle atmosphere circulation, but are currently very poorly constrained from observations.

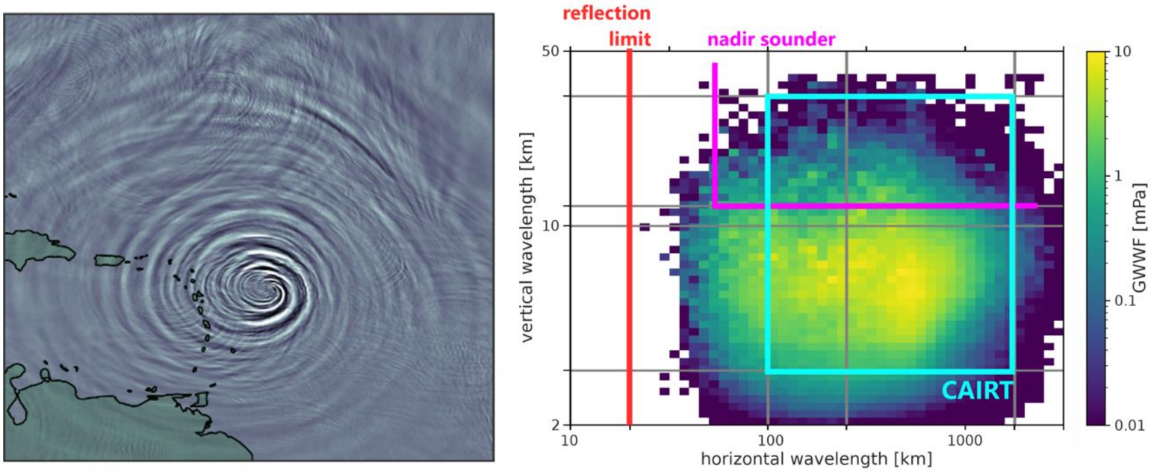

Figure 2. Atmospheric gravity waves. Left: An example of the gravity wave structure at 35 km altitude excited by the tropical cyclone Irma in September 2017, moving into the Caribbean, modelled by a high-resolution version of ECMWF's IFS model. Right: Global mean of gravity wave momentum flux for January 2006 as a function of horizontal and vertical wavelength, calculated from a high-resolution version (4.5 km grid spacing) of ECMWF's IFS model. A limb-imager like CAIRT with a sampling of 50 by 50 km horizontally and 1 km vertically could resolve a large fraction of the gravity wave momentum flux spectrum. Existing nadir sounders can detect only a small fraction of the total gravity wave momentum flux due to their reduced vertical resolution. The red line representing a 20 km horizontal wavelength marks the limit of wave propagation due to total reflection: waves with shorter wavelengths may exist, but they do not carry gravity wave momentum flux upward.

The CAIRT mission concept

The current lack of necessary observations motivated the CAIRT concept. The need to resolve gravity waves at the relevant wavelengths provides strong requirements for horizontal and vertical resolution. Figure 2 (left panel) shows as an example a numerical simulation of a gravity wave at about 30 km altitude that is excited by a tropical cyclone moving into the Caribbean. The right-hand panel shows the global mean spectrum of the gravity wave momentum flux for January 2006 from high resolution numerical simulations as a function of horizontal and vertical wavelength. Nadir sounders with their coarse vertical resolution can resolve only a small fraction of the relevant gravity wave spectrum (e.g., Hoffmann and Alexander, 2009). To capture the essential parts of the spectrum, wavelengths of 100 km

Accepted for publication in *Bulletin of the American Meteorological Society.* DOI 10.1175/BAMS-D-24-0217.1.

horizontally and 2-3 km vertically should be resolved, which requires a sampling of about 50 km horizontally and 1-2 km vertically, not achieved to date with existing sounders.

The observation principle of CAIRT is that of a Fourier-transform passive infrared limb-imaging spectrometer. In a single acquisition, the infrared limb emission will be observed simultaneously with an imaging detector over an altitude range of 4 to 115 km vertically and over about 400 km across track (300 – 500 km, depending on the yet-to-be-frozen technical concept), with an effective detector pixel size of about 1 km vertically and about 25 km horizontally (Figure 3). For each detector pixel an interferogram is recorded, which is then converted into a high-resolution spectrum. With acquisitions every 50 km along track of the satellite orbit, corresponding to an acquisition time of about 7 s, the individual observations can be combined in a tomographic retrieval, resulting in a spatial sampling of about 1 km vertically, 50 km horizontally along track and 25 km horizontally across track.

The along-track spacing of the individual acquisitions of 50 km and the corresponding acquisition time of 7 s provide strong technical constraints on the achievable detector readout speed and the interferogram maximum optical path length difference (OPD). With CAIRT's current technical concept, a Michelson interferometer with a maximum OPD of 2.5 cm, resulting in a spectral resolution of 0.2 cm^{-1} over a spectral range from 718 to 2200 cm^{-1}, is foreseen. Figure 4 provides example spectra, showing the spectral fingerprints of a large number of atmospheric constituents.

With a Michelson interferometer for passive infrared limb emission sounding, the CAIRT concept follows the heritage of the extremely successful MIPAS/Envisat mission (Fischer et al., 2008). The concept of infrared limb-imaging (Riese et al., 2005; Friedl-Vallon et al. 2006) has been successfully demonstrated by the GLORIA instrument (Riese et al., 2014; Friedl-Vallon et al., 2014) from aircraft and balloon flights since 2011. Through these heritage instruments, the CAIRT concept has a high technical and scientific maturity.

Tomographic retrievals will result in measurements of temperature and constituents on a nominal grid of 50 by 50 by 1 km, between 4 and 115 km vertically and a swath width of about 400 km across track, significantly exceeding the spatial sampling and vertical range of previous limb sounders. The actual effective spatial resolution will however depend on the signal-to-noise ratio of the individual data products. The list of CAIRT's primary Level-2 targets is shown in Table 1.

Accepted for publication in *Bulletin of the American Meteorological Society.* DOI 10.1175/BAMS-D-24-0217.1.

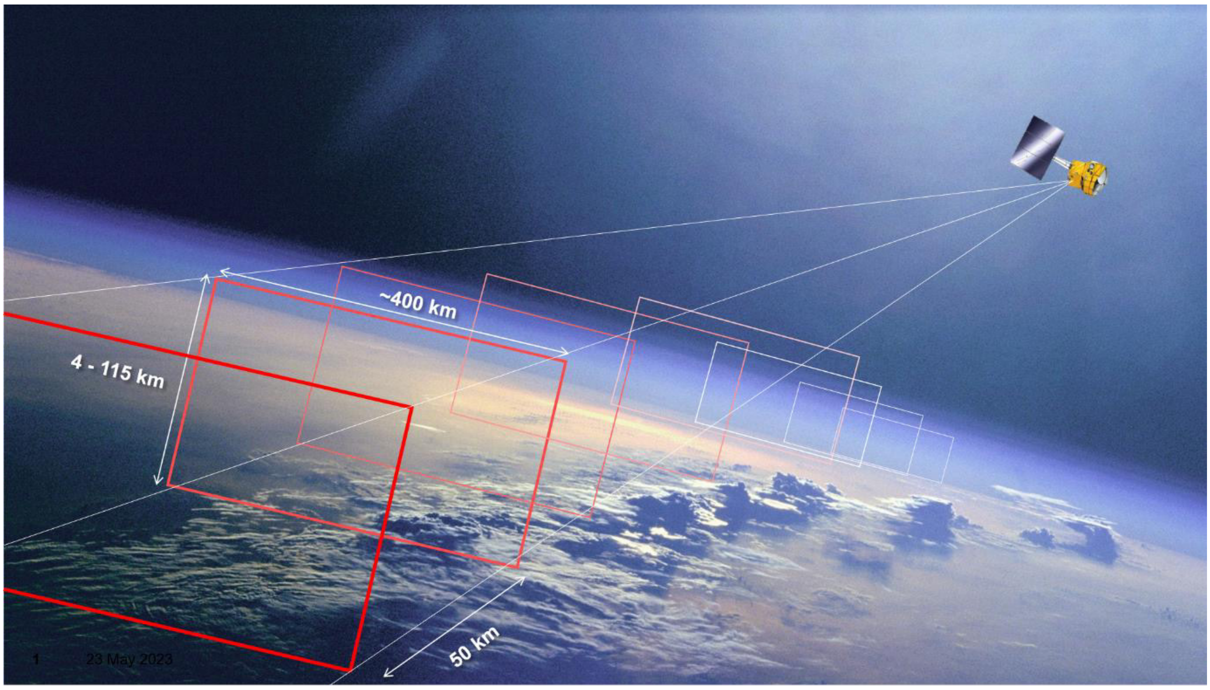

Figure 3. Illustration of the CAIRT observational concept. Every 50 km along track, corresponding to about every seven seconds, an infrared limb image with a tangent altitude range of 4 to 115 km and with about 400 km across track width is recorded. (Background image: NASA.)

Accepted for publication in *Bulletin of the American Meteorological Society.* DOI 10.1175/BAMS-D-24-0217.1.

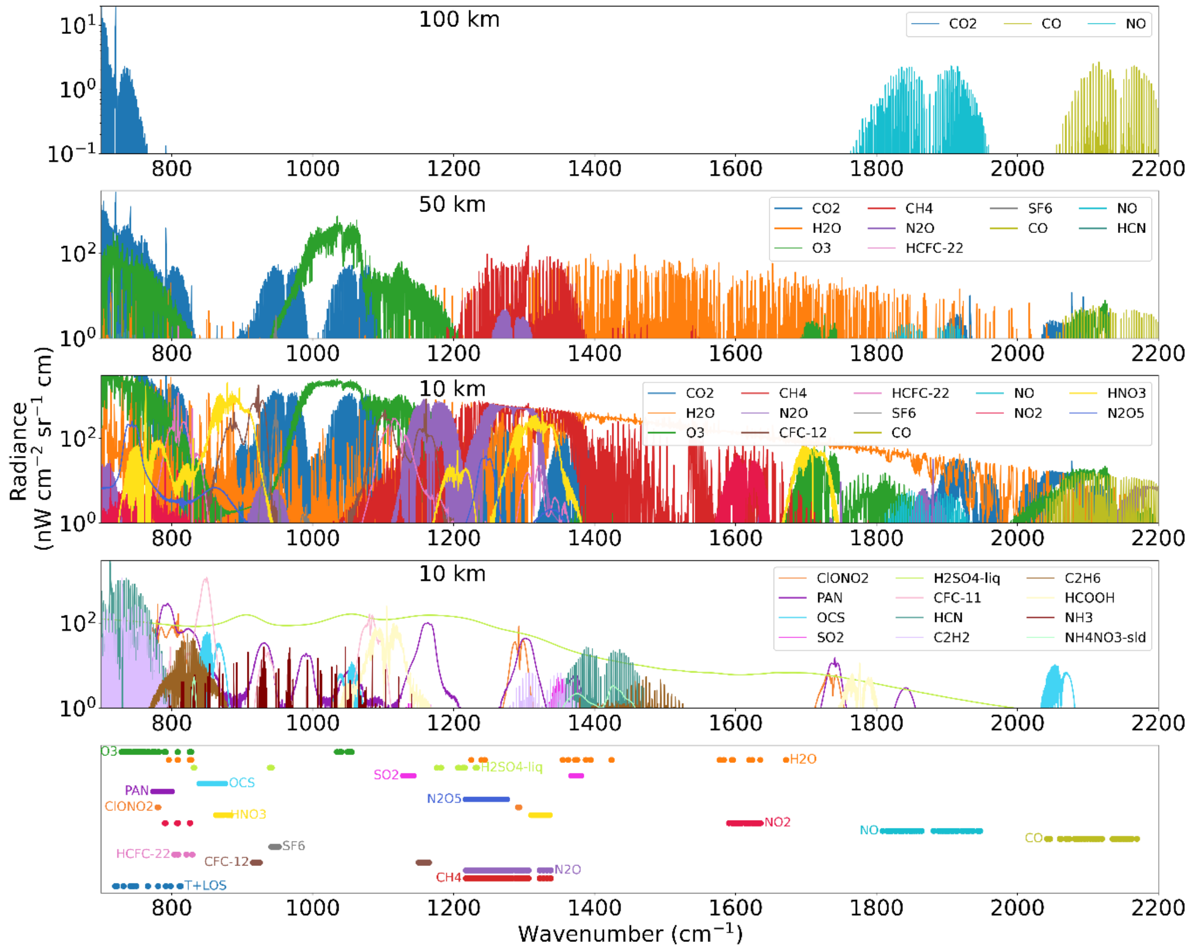

Figure 4. Calculated limb spectral radiances at 100 km (row 1), 50 km (row 2) and 10 km (rows 3 and 4) tangent point altitudes, for individual trace gases (reference atmosphere, 45°N, April). Bottom, approximate locations of retrieval micro-windows per target molecule, with "T+LOS" indicating temperature and line-of-sight.

Table 1. Primary Level-2 targets of the CAIRT mission concept.

Parameter	Vertical range
Temperature	Upper troposphere to lower thermosphere
Gravity wave amplitude, wavelength, phase speed, direction, and momentum flux	Stratosphere and mesosphere
Ozone	Upper troposphere to mesosphere
Water vapor	Upper troposphere to mesosphere

Accepted for publication in *Bulletin of the American Meteorological Society*. DOI 10.1175/BAMS-D-24-0217.1.

Long-lived tracers: SF_6, N_2O, CH_4, CFC-11, HCFC-22	Stratosphere
Age-of-air	Stratosphere
NO, CO	Lower stratosphere to lower thermosphere
Nitrogen compounds (NOy): NO, NO_2, HNO_3, N_2O_5, $ClONO_2$	Stratosphere
Sulfur budget: SO_2, H_2SO_4, COS	Upper troposphere and stratosphere
Pollutants: CO, PAN	Upper troposphere and lower stratosphere

Unique scientific contributions of infrared limb imaging

a. Resolving small scale structures in the middle atmosphere

As an example of small-scale structures in the middle atmosphere, Figure 5 shows a snapshot of ozone in the lower stratosphere from a high-resolution simulation of the Icosahedral Non-hydrostatic (ICON) model at 13 km grid spacing globally. These simulations show a great deal of small-scale structures and filaments at the 50 to 100 km scale, so far not available through regular observations at a global scale. This stirring, filamentation and quasi-horizontal mixing of tracers is an important part of the middle atmosphere transport circulation (Pierce and Fairlie, 1993; Dietmüller et al., 2017), but so far has not been well constrained by observations (e.g., Riese et al., 2012). Infrared limb imaging can close this observational gap.

Accepted for publication in *Bulletin of the American Meteorological Society.* DOI 10.1175/BAMS-D-24-0217.1.

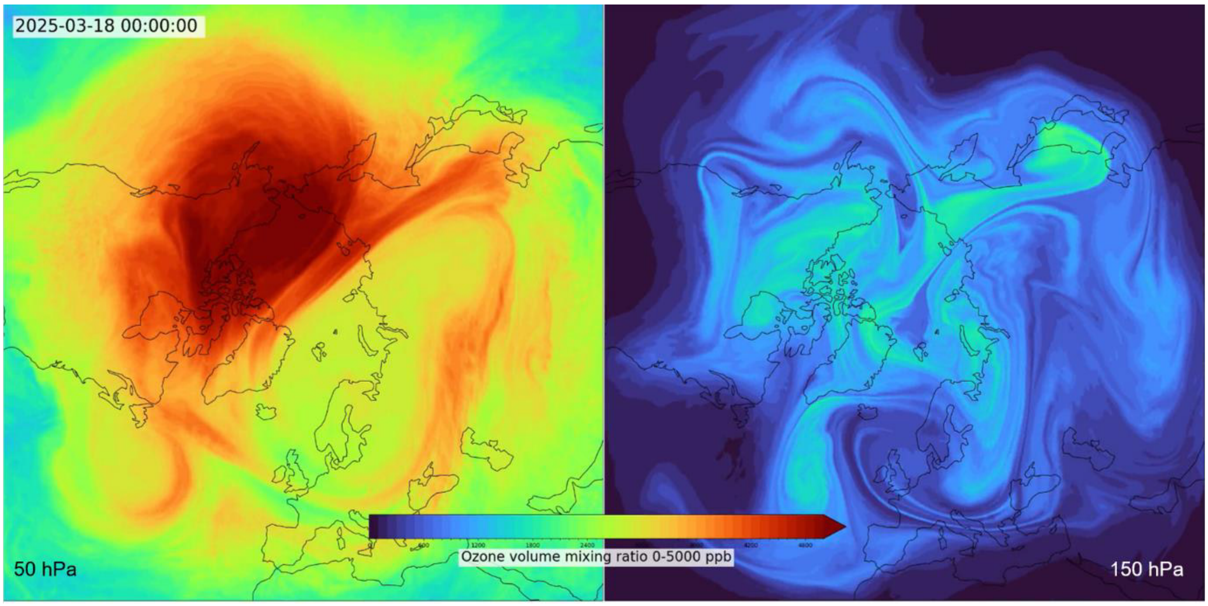

Figure 5. Modeled ozone distributions in the lower stratosphere at 50 hPa (left) and 150 hPa (right) for 18 March 2025. Simulations with the ICON model with 13 km grid spacing globally and a linearized ozone chemistry. Many small scale features at the 50 to 100 km scale are visible, to be resolved with infrared limb imaging along as well as across track.

b. Quantifying middle atmosphere age-of-air and circulation

Age-of-air is an important diagnostic of the strength of the meridional circulation in the stratosphere (e.g., Garny et al., 2025). Mean age-of-air can be calculated from tracer gases with a monotonic increase in surface concentrations, such as sulfur hexafluoride (SF_6). Previous infrared satellite observations by MIPAS/Envisat (2002-2012, Stiller et al. 2008; Stiller et al., 2012; Haenel et al., 2015) and ACE-FTS (Saunders et al., 2024) have provided time series of SF_6-derived age-of-air that can be continued into the future by an infrared limb imager like CAIRT. Because of the weak absorption features of SF_6, age-of-air derived from infrared limb measurements of SF_6 alone will likely require averaging over zonal means to achieve sufficient precision. Using additional long-lived tracers (such as N_2O and CFC-11), we have demonstrated that the studied concept can provide mean age-of-air on single observations at about 100 by 100 km horizontally and 1-2 km vertically with a total uncertainty less than 0.5 years and better than 0.25 years for zonal means (Voet et al., 2025; see also Ray et al., 2024). Such a multi-constituent approach would provide near-global observations of structures in age-of-air at scales that so far are accessible only by in-situ observations on campaign basis. These observations will help to better constrain the Brewer-Dobson circulation and long-term trends in the strength of the circulation since the 2010s (from MIPAS and ACE-FTS). The need for this type of observations to better constrain the

Accepted for publication in *Bulletin of the American Meteorological Society.* DOI 10.1175/BAMS-D-24-0217.1.

representation of the BDC in atmospheric reanalysis data, used for a range of climate applications, was also recently highlighted by major World Climate Research Programme (WCRP) reanalysis intercomparison activities (Monge-Sanz et al., 2022a).

c. Resolving gravity waves and quantifying the driving of the middle atmosphere circulation

Resolving the major part of the gravity wave spectrum with temperature observations at scales accessible with an infrared limb-imager (Figure 2) enables the derivation of representative gravity wave momentum flux and gravity wave drag distributions on a global scale. The gravity wave drag is the forcing of the background winds, and thereby, directly relates to the role of gravity waves in driving the middle atmosphere dynamics. A case study of the Northern Hemispheric (NH) 2006 sudden stratospheric warming (SSW) with synthetic CAIRT observations for January 2006 is shown in Figure 6, based on Rhode et al. (2024). Here, small-volume wave identification has been applied to simulated observations of temperature to characterize individual gravity waves along the satellite track in terms of their wavelengths and amplitude. This allows calculation of spatially resolved gravity wave momentum flux (Ern et al., 2004) along the orbit track as shown in Figure 6 (first row). The impact of the gravity waves on the large-scale dynamics is, however, seen more clearly in the zonal mean (second row): before the SSW (column a), negative gravity wave momentum flux is evenly distributed throughout the northern hemisphere stratosphere; during the SSW (panels b and c) gravity waves break below the wind reversal (i.e., the zero wind contour), resulting in a decrease in gravity wave momentum flux above due to breaking. We demonstrate that the high vertical resolution of CAIRT observations allows the estimation of gravity wave drag (calculated as the vertical gradient of gravity wave momentum flux; third row), directly showing the forcing effect of gravity waves on the wind. The gravity wave drag can also be calculated directly from the model's wind perturbations (fourth row). The simulated CAIRT observations show great correspondence to the model-derived drag, underscoring that infrared limb-imaging would give representative observations of gravity wave drag and even resolve small-scale structures.

Accepted for publication in *Bulletin of the American Meteorological Society.* DOI 10.1175/BAMS-D-24-0217.1.

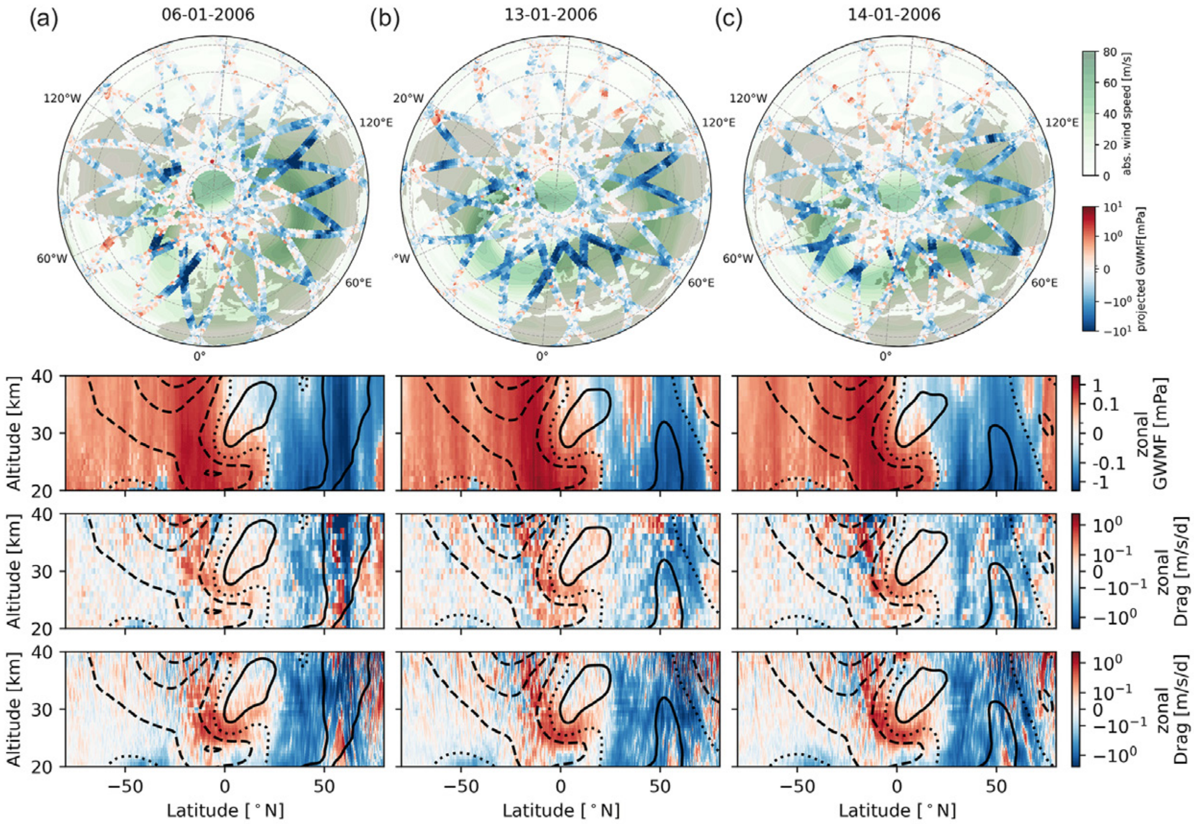

Figure 6. Maps of zonal gravity wave momentum flux (GWMF) at 25 km deduced from simulated CAIRT observations together with background wind speed (upper row), corresponding zonal-mean GWMF(second row) and drag (third row), and reference drag calculated from zonal-mean winds (fourth row). From left to right, the dates shown are 6, 13, and 14 January 2006. Contours of background wind in the zonal means are for 0 m s^{-1} (dotted) and 5, 10, 25, and 50 m s^{-1} for eastward (solid) and westward (dashed) winds. From Rhode et al. (2024) (CC 4.0).

Accepted for publication in *Bulletin of the American Meteorological Society.* DOI 10.1175/BAMS-D-24-0217.1.

d. Investigating the coupling with solar variability and space weather through the descent of NOy

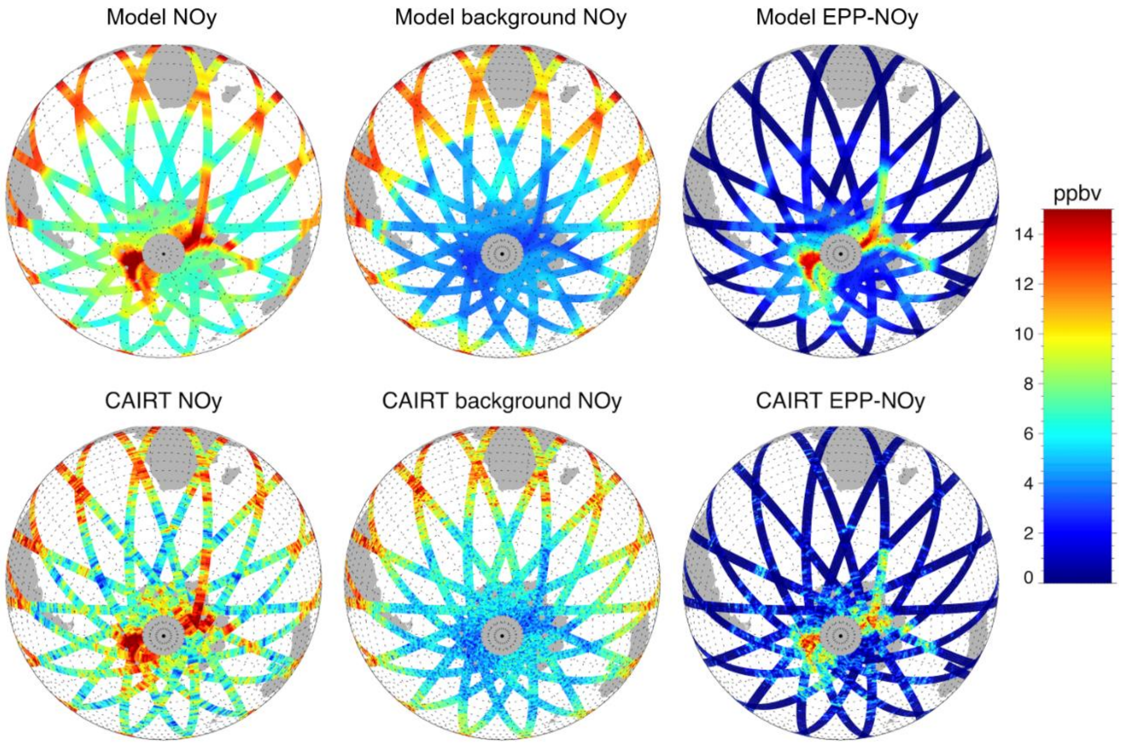

Figure 7. Quantifying the transport of reactive nitrogen compounds from the mesosphere/lower thermosphere into the stratosphere. Total NO_y (left), and separate contributions from the stratospheric background NO_y (middle) and descending EPP-NO_y (right), in the SH at 50 km altitude on 14 June 2022. Plots show model truth (top) and synthetic CAIRT retrieved data (bottom), considering random and systematic measurement error sources.

Space-weather-driven auroral NO production by energetic particles peaks around 105 km altitude, but with pronounced spatial and temporal variability. Synthetic CAIRT observations reproduce the distribution of the enhanced NO layer with high fidelity, even above the vertical limit of the observations (above the instrument's field of view). This is possible because of the tomographic retrieval approach, making use of and correctly locating the information from NO emissions originating at higher altitudes. The capacity of an infrared limb imager to quantify the flux of reactive nitrogen (NOy) produced by energetic particles (EPPNOy) into the stratosphere during polar winters is demonstrated here for the 2022 SH winter (Figure 7). Tracer correlations (NOy-CO, NOy-CH_4) are used to distinguish the descending NOy contribution from the stratospheric background produced from N_2O oxidation. The quality of the inferred tracer correlations and hence the accuracy of the NOy

Accepted for publication in *Bulletin of the American Meteorological Society.* DOI 10.1175/BAMS-D-24-0217.1.

contribution from the upper atmosphere that can be determined depends strongly on the accuracy and vertical resolution of the retrieved abundances (Funke et al., 2014). EPP-NO_y extracted using tracer correlations from the retrieval simulations and from the model are shown in Figure 7. We see that data from an instrument like CAIRT would enable a quantification of the particle-produced NOy in the stratosphere.

e. Detecting the input of aerosols and pollutants

Biomass burning can input considerable amounts of aerosols into the lower stratosphere, leading to a dimming of solar radiation exceeding the effects of medium-sized volcanic eruptions (Khaykin et al., 2020), with an additional localized radiative heating due to carbon-containing aerosol absorption of solar radiation (Sellitto et al., 2023). Furthermore, the input of biomass burning aerosols and pollutants may lead to depletion of stratospheric ozone (Solomon et al., 2023).

With a relatively high spectral resolution, infrared limb-imaging can detect and quantify pollutants and aerosols in the UTLS, following the heritage of previous instruments such as MIPAS/Envisat (e.g., Glatthor et al., 2007; Glatthor et al., 2009; Höpfner et al., 2019; Glatthor et al., 2025) or ACE-FTS (e.g., Bernath et al., 2023), but with higher spatial resolution. Improved spatial resolution enhances the probability of detecting plumes with small vertical or horizontal extent. As an example, Figure 8 shows a biomass burning plume of peroxyacetyl nitrate (PAN) observed from the airborne limb-imager demonstrator GLORIA in the UTLS over the South Atlantic (Johansson et al., 2022), compared here to synthetic CAIRT observations of the same plume based on the Copernicus Atmospheric Monitoring System (CAMS) analyses.

Moreover, future infrared limb observations would offer the unique capability to close the stratospheric sulfur budget (e.g., Kremser et al., 2016; Günther et al., 2018; Brodowsky et al., 2024), by observing simultaneously the mass of stratospheric sulfate aerosols, together with the most important gas phase precursors carbonyl sulfide (COS) and sulfur dioxide (SO_2). This is also of particular relevance to investigate the unintended and unexpected side effects of proposed solar radiation management by the deliberate injection of aerosols into the stratosphere before this is attempted (e.g., National Academy of Sciences, 2021).

Accepted for publication in *Bulletin of the American Meteorological Society.* DOI 10.1175/BAMS-D-24-0217.1.

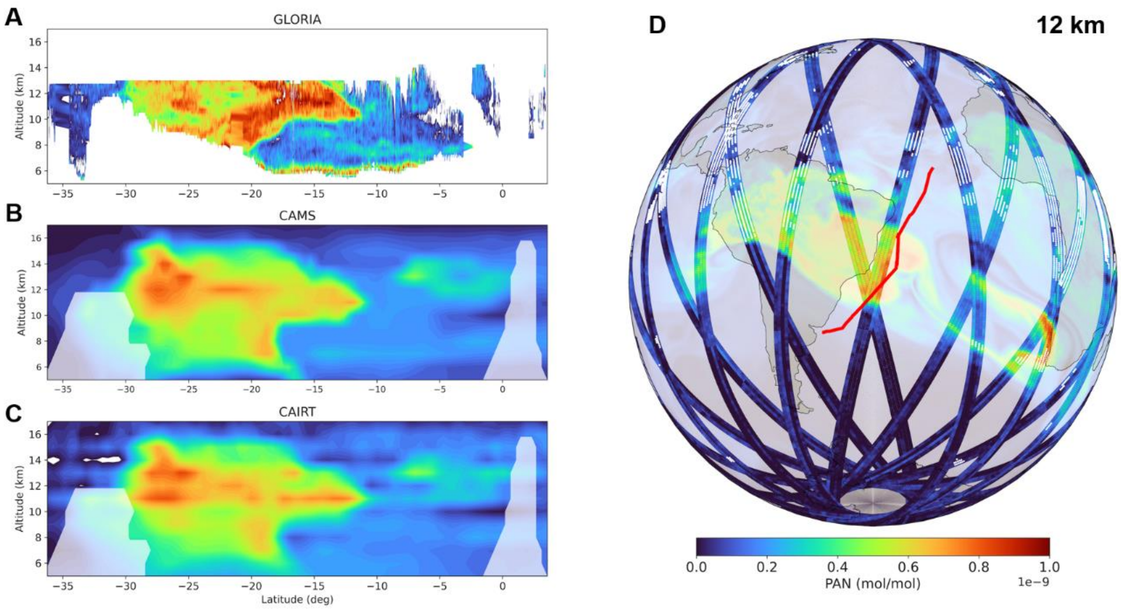

Figure 8. Observation of a biomass burning plume of enhanced peroxyacetyl nitrate (PAN) in the UTLS from the GLORIA airborne instrument over the South Atlantic (Panel A, Johansson et al., 2022). The corresponding analysis from the Copernicus Atmospheric Monitoring System (CAMS) is shown in Panel B, while Panel C shows synthetic CAIRT observations based on the CAMS analysis. Panel D shows the synthetic CAIRT observations at 12 km altitude for one day, with the CAMS analysis in the background. White areas in panels B-D indicate the presence of modelled clouds, that can be compared to observed clouds (missing data/white areas below flight altitude in panel A).

f. Ozone and water vapor in the tropopause region and stratosphere-troposphere exchange

Ozone and water vapor are important greenhouse gases, with changes around the tropopause having a particularly large radiative efficiency for the forcing of surface climate (Riese et al., 2012). Transport from the stratosphere into the troposphere is a significant source of tropospheric ozone, where it acts as an important greenhouse gas and affects air quality (e.g., Griffiths et al., 2021; IPCC, 2023). Model simulations predict an increase in the flux of ozone into the troposphere as a result of changes in the strength of the Brewer-Dobson circulation and the recovery of stratospheric ozone (Hegglin and Shepherd, 2009; Meul et al., 2018). Quantifying the stratosphere-to-troposphere flux of ozone from observations is still associated with large uncertainties. Future limb observations are needed to improve this by providing accurate and high-resolution observations of ozone and water vapor in the upper troposphere and lower stratosphere. This capability has been evaluated using an observing system simulation experiment (OSSE) where CAIRT synthetic observations have been simulated taking the CAMS control simulation as references, these observations being

Accepted for publication in *Bulletin of the American Meteorological Society.* DOI 10.1175/BAMS-D-24-0217.1.

assimilated by the BASCOE system (Errera et al., 2021; Errera et al., 2025). Figure 9 compares the assimilation run against the reference, as well as a control run (without data assimilation) and an assimilation run of synthetic MLS observations. The OSSE indicates that observations from an infrared limb-imager like CAIRT are expected to be an improvement in the capacity to constrain ozone and water vapor around the tropopause compared to the current MLS-based methods.

A moist bias in the lower stratosphere is a common feature across many numerical weather prediction (e.g., Bland et al., 2024; Woiwode et al., 2020; Krüger et al., 2022) and climate models (Charlsworth et al., 2023). This moist bias leads to a modeled cold bias in the extra-tropical lowermost stratosphere (e.g., Bland et al., 2024), affecting atmospheric circulation and dynamics down into the troposphere (Lawrence at al., 2022; Charlsworth et al., 2023). The ability of future infrared limb observations to provide precise water vapor observations at high spatial resolution around the tropopause with its strong gradients in humidity will thus be very beneficial.

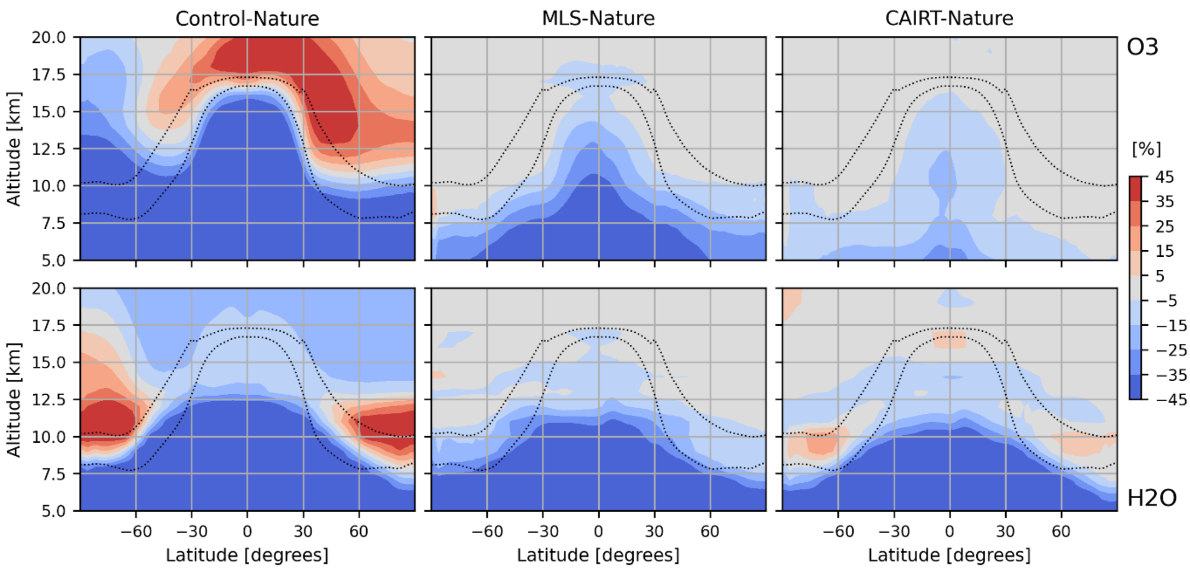

Figure 9. Results from an observation system simulation experiment (OSSE), comparing the assimilation of ozone and water vapor from the Microwave Limb Sounder (MLS) and pseudo-observations from CAIRT. Left: bias of the BASCOE model control run without assimilation for the period Oct 2021 to Feb 2022 to the reference simulation. Middle: bias of the model with MLS data assimilated. Right: bias of model with assimilation of synthetic CAIRT data. Dashed lines represent the tropopause layer.

Accepted for publication in *Bulletin of the American Meteorological Society.* DOI 10.1175/BAMS-D-24-0217.1.

g. Limb-nadir synergies

Infrared limb observations provide high vertical resolution in the middle atmosphere and upper troposphere, but cannot deliver much information in the lower troposphere due to the presence of clouds and increased opacity from water vapor. Even under optimal conditions, little information could be obtained below about four kilometers altitude. Nadir observations on the other hand have much coarser vertical resolution in the UTLS, but can under clear-sky conditions provide information also on the lower troposphere, with fine horizontal resolution. It has been shown that the combination of limb observations and multiple nadir observations covering the region of the limb lines of sight can provide synergistic retrievals of trace gases with improved performances in terms of both spatial resolution and uncertainties throughout the troposphere and lower stratosphere (Tirelli et al., 2025). The complementarity between limb and nadir observations could be exploited not only for trace gas retrieval but also for clouds and volcanic plumes, with limb observations providing unique information on the vertical extension of also very thin clouds and plumes, while nadir measurements provide information on other physical properties of the clouds.

h. Improving Numerical Weather Prediction

Most weather forecasting centers have raised their model top altitude well into the upper stratosphere or even mesosphere to improve forecast skill. However, there are at present few observations above the lower stratosphere to constrain models in that region.

Improving the representation of water vapor and ozone in the upper troposphere and lower stratosphere in numerical weather forecasting models has been shown to lead to significant improvements in meteorological predictions (Hogan et al., 2017; Monge-Sanz et al., 2022b). Assimilation of water vapor data from MLS in ECMWF's forecasting system resulted in significant improvements (Semane and Bonavita, 2025). In addition, first tests in direct assimilation of infrared limb radiance from MIPAS/Envisat into ECMWF's forecasting system were very encouraging (Bormann et al., 2007). Future limb observations of infrared radiances and selected level-2 products (temperature, ozone, and water vapor) should therefore be considered for operational weather and air quality forecasts.

Limb observations of absolute GWMF have already been used to constrain the gravity wave parametrization in the ECWMF model (Orr et al. 2010), and were later implemented also in the ICON model at the Deutscher Wetterdienst (DWD). The additional information provided

Accepted for publication in *Bulletin of the American Meteorological Society.* DOI 10.1175/BAMS-D-24-0217.1.

by infrared limb-imaging would also allow the constraint of source-specific parametrizations like the convective gravity wave scheme (Richter et al. 2010) used in the Whole Atmosphere Community Climate Model (WACCM).

There is currently a revolution in the use of Artificial Intelligence (AI) models for weather and climate prediction (e.g., de Burgh-Day and Leeuwenburg, 2023). AI methods for constructing analyses and forecasts directly from satellite observations without the need for data assimilation are currently being explored, but still in their infancies (e.g. Keller and Pothast, 2024; McNally et al., 2024). It is very difficult to predict how this field will develop in the coming years, but with the large amount of unique data in the middle atmosphere not available from any other observations, future infrared limb-imaging will likely be of high relevance for developing data-driven atmospheric models.

Concluding remarks

The middle atmosphere is at the nexus of the atmospheric climate system, connecting the lower atmosphere above the Earth's surface with the upper atmosphere and near-space environment that is under the influence of space weather and solar variability. The middle atmosphere is strongly affected by increasing concentrations of greenhouse gases, the recovery from ozone-depleting substances, the expected rise in impacts from biomass burning, and spacecraft launches and reentries. Accordingly, we are entering uncharted territory in the coming decades. The unwanted side effects of proposed solar radiation management by the deliberate injection of aerosols into the stratosphere are not well understood and require monitoring and further understanding of the middle atmosphere. Yet the present observational capacity to detect, attribute and understand the expected changes in the middle atmosphere is severely limited. New infrared limb-imaging technology will provide the data needed to address these challenges and to provide a step-change in our understanding of the middle atmosphere. We have investigated this with the proposed CAIRT concept. The CAIRT concept already has a high level of technological and scientific readiness, based on the heritage of the airborne instrument GLORIA and extensive performance and impact assessment studies, performed as part of the ESA Earth Explorer program. The high spatial resolution observations provide much needed information on atmospheric gravity waves, their sources, pathways and driving of the atmospheric circulation, one of the largest uncertainties in models at present. By simultaneously observing the middle atmosphere from the upper troposphere up to the lower thermosphere, infrared

Accepted for publication in *Bulletin of the American Meteorological Society.* DOI 10.1175/BAMS-D-24-0217.1.

limb-imaging provides a whole atmosphere view of the coupling between atmospheric composition, circulation and climate change.

Acknowledgments.

Parts of this work were supported by ESA through the contracts "CAIRT SciReC", "CAIRT PerReC", "MAGIC4AMPAC", and "CAIRTEX". PS acknowledges funding by CNES through the project "EXTRA-SAT". High resolution ICON model simulations were performed by Luca Reißig, with financial support by the German Science Foundation (DFG) through grant "SI 1400/5-1".

Data Availability Statement.

ICON model output can be obtained upon request to bjoern-martin.sinnhuber@kit.edu. BASCOE runs can be obtained upon request to quentin.errera@aeronomie.be.

REFERENCES

Abalos, M., Polvani, L., Calvo, N., Kinnison, D., Ploeger, F., Randel, W., and Solomon, S., 2019: New insights on the impact of ozone-depleting substances on the Brewer-Dobson circulation, *J. Geophys. Res. Atmospheres*, **124**, 2435–2451, https://doi.org/10.1029/2018JD029301.

Alexander, M.J., Geller, M., McLandress, C., Polavarapu, S., Preusse, P., Sassi, F., Sato, K., Eckermann, S., Ern, M., Hertzog, A., Kawatani, Y.A., Pulido, M., Shaw, T., Sigmond, M., Vincent, R., Watanabe, S., 2010: Recent developments in gravity-wave effects in climate models and the global distribution of gravity-wave momentum flux from observations and models, *Q. J. R. Meteorol. Soc.*, **136**, 1103–1124, https://doi.org/0.1002/qj.637

Añel, J. A., Cnossen, I., Antuña-Marrero, J. C., Beig, G., Brown, M. K., Doornbos, E., et al., 2025: The need for better monitoring of climate change in the middle and upper atmosphere, *AGU Advances,* **6**, e2024AV001465. https://doi.org/10.1029/2024AV001465.

Bernath, P., Boone, C., and Crouse, J., 2022: Wildfire smoke destroys stratospheric ozone, *Science*, **375**, 1292–1295, https://doi.org/10.1126/science.abm5611.

Accepted for publication in *Bulletin of the American Meteorological Society.* DOI 10.1175/BAMS-D-24-0217.1.

Bland, J., R. Forbes, S. L. Gray, and J. Methven, 2024: Processes controlling extratropical near-tropopause humidity and temperature in the ECMWF global weather forecast model, *Q. J. Royal Met. Soc.*, https://doi.org/10.1002/qj.4873.

Bormann, N., and J.-N. Thépaut, 2007: Assimilation of MIPAS limb radiances in the ECMWF system. I: Experiments with a 1-dimensional observation operator, *Q. J. Royal Met. Soc*, https://doi.org/10.1002/qj.46.

Brodowsky, C. V., Sukhodolov, T., Chiodo, G., Aquila, V., Bekki, S., Dhomse, S. S., Höpfner, M., Laakso, A., Mann, G. W., Niemeier, U., Pitari, G., Quaglia, I., Rozanov, E., Schmidt, A., Sekiya, T., Tilmes, S., Timmreck, C., Vattioni, S., Visioni, D., Yu, P., Zhu, Y., and Peter, T., 2024: Analysis of the global atmospheric background sulfur budget in a multi-model framework, *Atmos. Chem. Phys.*, **24**, 5513–5548, https://doi.org/10.5194/acp-24-5513-2024.

Butchart, N., 2014: The Brewer-Dobson circulation, *Rev. Geophys*., **52**, 157–184, https://doi.org/10.1002/2013RG000448.

Butchart, N., and A. Scaife, 2001: Removal of chlorofluorocarbons by increased mass exchange between the stratosphere and troposphere in a changing climate, *Nature* **410**, 799–802, https://doi.org/10.1038/35071047.

Butler, A., et al., 2019: Sub-seasonal predictability and the stratosphere, in: Sub-seasonal to seasonal prediction: The gap between weather and climate forecasting, edited by: Robertson, A. W. and Vitart, F., Elsevier, Amsterdam, Kidlington, Cambridge, 223–241, https://doi.org/10.1016/B978-0-12-811714-9.00011-5.

de Burgh-Day, C. O. and Leeuwenburg, T., 2023: Machine learning for numerical weather and climate modelling: a review, *Geosci. Model Dev.*, **16**, 6433–6477, https://doi.org/10.5194/gmd-16-6433-2023.

Charlesworth, E., Plöger, F., Birner, T., Baikhadzhaev, R., Abalos, M., Abraham, N. L., Akiyoshi, H., Bekki, S., Dennison, F., Jöckel, P., Keeble, J., Kinnison, D., Morgenstern, O., Plummer, D., Rozanov, E., Strode, S., Zeng, G., Egorova, T., and Riese, M., 2023: Stratospheric water vapour affecting atmospheric circulation, *Nat. Commun.*, **14**, 3925, https://doi.org/10.1038/s41467-023-39559-2.

Chipperfield, M.P., Liang, Q., Strahan, S. E., Morgenstern, O., Dhomse, S. S., Abraham, N. L., Archibald, A. T., Bekki, S., Braesicke, P., Di Genova, G., Fleming, E. L., Hardiman,

Accepted for publication in *Bulletin of the American Meteorological Society.* DOI 10.1175/BAMS-D-24-0217.1.

S. C., Iachetti, D., Jackman, C. H., Kinnison, D. E., Marchand, M., Pitari, G., Pyle, J. A., Rozanov, E., Stenke, A. and Tummon, F., 2014: Multi-model estimates of atmospheric lifetimes of long-lived Ozone-Depleting Substances: Present and future, *J. Geophys. Res.*, **119**, 2555-2573, https://doi.org/10.1002/2013JD021097.

Chipperfield, M. P. and Bekki, S., 2024: Opinion: Stratospheric ozone – depletion, recovery and new challenges, *Atmos. Chem. Phys.*, **24**, 2783–2802, https://doi.org/10.5194/acp-24-2783-2024.

Crevoisier, C., Clerbaux, C., Guidard, V., Phulpin, T., Armante, R., Barret, B., Camy-Peyret, C., Chaboureau, J.-P., Coheur, P.-F., Crépeau, L., Dufour, G., Labonnote, L., Lavanant, L., Hadji-Lazaro, J., Herbin, H., Jacquinet-Husson, N., Payan, S., Péquignot, E., Pierangelo, C., Sellitto, P., and Stubenrauch, C., 2014: Towards IASI-New Generation (IASI-NG): impact of improved spectral resolution and radiometric noise on the retrieval of thermodynamic, chemistry and climate variables, *Atmos. Meas. Tech.,* **7**, 4367–4385, https://doi.org/10.5194/amt-7-4367-2014.

Dhomse, S. S., Kinnison, D., Chipperfield, M. P., Salawitch, R. J., Cionni, I., Hegglin, M. I., Abraham, N. L., Akiyoshi, H., Archibald, A. T., Bednarz, E. M., Bekki, S., Braesicke, P., Butchart, N., Dameris, M., Deushi, M., Frith, S., Hardiman, S. C., Hassler, B., Horowitz, L. W., Hu, R.-M., Jöckel, P., Josse, B., Kirner, O., Kremser, S., Langematz, U., Lewis, J., Marchand, M., Lin, M., Mancini, E., Marécal, V., Michou, M., Morgenstern, O., O'Connor, F. M., Oman, L., Pitari, G., Plummer, D. A., Pyle, J. A., Revell, L. E., Rozanov, E., Schofield, R., Stenke, A., Stone, K., Sudo, K., Tilmes, S., Visioni, D., Yamashita, Y., and Zeng, G., 2018: Estimates of ozone return dates from Chemistry-Climate Model Initiative simulations, *Atmospheric Chem. Phys.,* **18**, 8409–8438, https://doi.org/10.5194/acp-18-8409-2018.

Dietmüller, S., Garny, H., Plöger, F., Jöckel, P., and Cai, D., 2017: Effects of mixing on resolved and unresolved scales on stratospheric age of air, *Atmos. Chem. Phys.*, **17**, 7703–7719, https://doi.org/10.5194/acp-17-7703-2017.

Ern, M., P. Preusse, M. J. Alexander, and C. D. Warner, 2004: Absolute values of gravity wave momentum flux derived from satellite data, *J. Geophys. Res.,* **109**, D20103, doi:10.1029/2004JD004752.

Accepted for publication in *Bulletin of the American Meteorological Society.* DOI 10.1175/BAMS-D-24-0217.1.

Errera, Q., Dekemper, E., Baker, N., Debosscher, J., Demoulin, P., Mateshvili, N., Pieroux, D., Vanhellemont, F., and Fussen, D., 2021: On the capability of the future ALTIUS ultraviolet–visible–near-infrared limb sounder to constrain modelled stratospheric ozone, *Atmos. Meas. Tech.*, **14**, 4737–4753, https://doi.org/10.5194/amt-14-4737-2021.

Errera, Q., Op de beeck, M., Bender, S., Flemming, J., Funke, B., Hoffmann, A., Höpfner, M., Livesey, N., Poli, G., Pieroux, D., Raspollini, P., and Sinnhuber, B.-M., 2025: On the capability of the Changing Atmosphere Infra-Red Tomography explorer (CAIRT) candidate mission to constrain O_3 and H_2O in the upper troposphere and lower stratosphere, EGUsphere, https://doi.org/10.5194/egusphere-2025-6130, 2025.

Ferreira, J. P., Z. Huang, K. Nomura, and J. Wang, 2024: Potential ozone depletion from satellite demise during atmospheric reentry in the era of mega-constellations, *Geophys. Res. Lett.*, **51**, https://doi.org/10.1029/2024GL109280.

Fischer, H., Birk, M., Blom, C., Carli, B., Carlotti, M., von Clarmann, T., Delbouille, L., Dudhia, A., Ehhalt, D., Endemann, M., Flaud, J. M., Gessner, R., Kleinert, A., Koopman, R., Langen, J., López-Puertas, M., Mosner, P., Nett, H., Oelhaf, H., Perron, G., Remedios, J., Ridolfi, M., Stiller, G., and Zander, R., 2008: MIPAS: an instrument for atmospheric and climate research, *Atmos. Chem. Phys.*, **8**, 2151–2188, https://doi.org/10.5194/acp-8-2151-2008.

Friedl-Vallon, F., M. Riese, G. Maucher, A. Lengel, F. Hase, P. Preusse, R. Spang, 2006: Instrument concept and preliminary performance analysis of GLORIA, *Advances in Space Research,* **37**, 2287-2291, ISSN 0273-1177, https://doi.org/10.1016/j.asr.2005.07.075.

Friedl-Vallon, F., T. Gulde, F. Hase, A. Kleinert, T. Kulessa, G. Maucher, T. Neubert, F. Olschewski, C. Piesch, P. Preusse, H. Rongen, C. Sartorius, H. Schneider, A. Schönfeld, V. Tan, N. Bayer, J. Blank, R. Dapp, A. Ebersoldt, H. Fischer, F. Graf, T. Guggenmoser, M. Höpfner, M. Kaufmann, E. Kretschmer, T. Latzko, H. Nordmeyer, H. Oelhaf, J. Orphal, M. Riese, G. Schardt, J. Schillings, M. K. Sha, O. Suminska-Ebersoldt, and J. Ungermann, 2014: Instrument concept of the imaging Fourier transform spectrometer GLORIA, *Atmos. Meas. Tech.*, **7**, 3565-3577, doi:10.5194/amt-7-3565-2014.

Accepted for publication in *Bulletin of the American Meteorological Society.* DOI 10.1175/BAMS-D-24-0217.1.

Funke, B., López-Puertas, M., Stiller, G. P., and von Clarmann, T., 2014: Mesospheric and stratospheric NOy produced by energetic particle precipitation during 2002-2012, *J Geophys Res*, **119**, https://doi.org/10.1002/2013JD021404.

Garny, H., Ploeger, F., Abalos, M., Bönisch, H., Castillo, A.E., von Clarmann, T., Diallo, M., Engel, A., Laube, J.C., Linz, M., Neu, J.L., Podglajen, A., Ray, E., Rivoire, L., Saunders, L.N., Stiller, G., Voet, F., Wagenhäuser, T., Walker, K.A., 2024: Age of stratospheric air: progress on processes, observations, and long-term trends, *Rev. Geophys.*, **62**, e2023RG000832. https://doi.org/10.1029/2023RG000832.

Glatthor, N., von Clarmann, T., Fischer, H., Funke, B., Grabowski, U., Höpfner, M., Kellmann, S., Kiefer, M., Linden, A., Milz, M., Steck, T., and Stiller, G. P., 2007: Global peroxyacetyl nitrate (PAN) retrieval in the upper troposphere from limb emission spectra of the Michelson Interferometer for Passive Atmospheric Sounding (MIPAS), *Atmos. Chem. Phys.*, **7**, 2775–2787, https://doi.org/10.5194/acp-7-2775-2007.

Glatthor, N., von Clarmann, T., Stiller, G. P., Funke, B., Koukouli, M. E., Fischer, H., Grabowski, U., Höpfner, M., Kellmann, S., and Linden, A., 2009: Large-scale upper tropospheric pollution observed by MIPAS HCN and C_2H_6 global distributions, *Atmos. Chem. Phys.*, **9**, 9619–9634, https://doi.org/10.5194/acp-9-9619-2009.

Glatthor, N., G. P. Stiller, T. von Clarmann, B. Funke, S. Kellmann, and A. Linden, 2025: Upper-tropospheric pollutants observed by MIPAS: geographic and seasonal variations, *Atmos. Chem. Phys.*, **25**, 1175–1208, https://doi.org/10.5194/acp-25-1175-2025.

Global Climate Observing System (GCOS), 2022: The 2022 GCOS ECVs Requirements (GCOS-245), GCOS, Geneva.

Griffiths, P. T., Murray, L. T., Zeng, G., Shin, Y. M., Abraham, N. L., Archibald, A. T., Deushi, M., Emmons, L. K., Galbally, I. E., Hassler, B., Horowitz, L. W., Keeble, J., Liu, J., Moeini, O., Naik, V., O'Connor, F. M., Oshima, N., Tarasick, D., Tilmes, S., Turnock, S. T., Wild, O., Young, P. J., and Zanis, P., 2021: Tropospheric ozone in CMIP6 simulations, *Atmos. Chem. Phys.*, **21**, https://doi.org/10.5194/acp-21-4187-2021.

Günther, A., Höpfner, M., Sinnhuber, B.-M., Griessbach, S., Deshler, T., von Clarmann, T., and Stiller, G., 2018: MIPAS observations of volcanic sulfate aerosol and sulfur dioxide in the stratosphere, *Atmos. Chem. Phys.*, **18**, 1217–1239, https://doi.org/10.5194/acp-18-1217-2018.

Accepted for publication in *Bulletin of the American Meteorological Society.* DOI 10.1175/BAMS-D-24-0217.1.

Haenel, F., Stiller, G. P., von Clarmann, T., Funke, B., Eckert, E., Glatthor, N., Grabowski, U., Kellmann, S., Kiefer, M., Linden, A., and Reddmann, T., 2015: Reassessment of MIPAS age of air trends and variability, *Atmos. Chem. Phys.*, **22**, 13 161–13 176, https://doi.org/10.5194/acp-15-13161-2015.

Hegglin, M., and Shepherd, T. G., 2009: Large climate-induced changes in ultraviolet index and stratosphere-to-troposphere ozone flux, *Nature Geosci.,* **2**, 687–691, https://doi.org/10.1038/ngeo604.

Höpfner, M., Ungermann, J., Borrmann, S. et al, 2019: Ammonium nitrate particles formed in upper troposphere from ground ammonia sources during Asian monsoons, *Nat. Geosci.* **12**, 608–612, https://doi.org/10.1038/s41561-019-0385-8.

Hoffmann, L. and Alexander, M. J., 2009: Retrieval of stratospheric temperatures from Atmospheric Infrared Sounder radiance measurements for gravity wave studies, *J. Geophys. Res.*, **114**, D07105, https://doi.org/10.1029/2008JD011241.

Hogan, R. J., et al., 2017: Radiation in numerical weather prediction, *ECMWF Technical Memorandum*, **816**.

Intergovernmental Panel on Climate Change (IPCC) (Ed.), 2023: Short-lived Climate Forcers, in: Climate Change 2021 – The Physical Science Basis: Working Group I Contribution to the Sixth Assessment Report of the Intergovernmental Panel on Climate Change, Cambridge University Press, Cambridge, 817–922, https://doi.org/10.1017/9781009157896.008.

Johansson, S., Wetzel, G., Friedl-Vallon, F., Glatthor, N., Höpfner, M., Kleinert, A., Neubert, T., Sinnhuber, B.-M., and Ungermann, J., 2022: Biomass burning pollution in the South Atlantic upper troposphere: GLORIA trace gas observations and evaluation of the CAMS model, *Atmos. Chem. Phys.*, **22**, 3675–3691, https://doi.org/10.5194/acp-22-3675-2022.

Keeble, J., et al., 2021: Evaluating stratospheric ozone and water vapour changes in CMIP6 models from 1850 to 2100, *Atmos. Chem. Phys.*, **21**, 5015–5061, https://doi.org/10.5194/acp-21-5015-2021.

Keller, J. D., and Potthast, R., 2024: AI-based data assimilation: Learning the functional of analysis estimation. *arXiv preprint arXiv:2406.00390*.

Accepted for publication in *Bulletin of the American Meteorological Society.* DOI 10.1175/BAMS-D-24-0217.1.

Khaykin, S., Legras, B., Bucci, S., Sellitto, P., Isaksen, L., Tencé, F., Bekki, S., Bourassa, A., Rieger, L., Zawada, D., Jumelet, J., and Godin-Beekmann, S., 2020: The 2019/20 Australian wildfires generated a persistent smoke-charged vortex rising up to 35 km altitude, *Commun. Earth Environ.,* 1, **22**, https://doi.org/10.1038/s43247-020-00022-5.

Kidston, J., Scaife, A. A., Hardiman, S. C., Mitchell, D. M., Butchart, N., Baldwin, M. P., and Gray, L. J., 2015: Stratospheric influence on tropospheric jet streams, storm tracks and surface weather, *Nat. Geosci.,* **8**, 433–440, https://doi.org/10.1038/ngeo2424.

King, A. D., Butler, A. H., Jucker, M., Earl, N. O., and Rudeva, I., 2019: Observed relationships between sudden stratospheric warmings and European climate extremes, *J. Geophys. Res. Atmospheres,* **124**, 13943–13961, https://doi.org/10.1029/2019JD030480.

Kremser, S., Thomason, L. W., von Hobe, M., Hermann, M., Deshler, T., Timmreck, C., Toohey, M., Stenke, A., Schwarz, J. P., Weigel, R., Fueglistaler, S., Prata, F. J., Vernier, J.-P., Schlager, H., Barnes, J. E., Antuña-Marrero, J.-C., Fairlie, D., Palm, M., Mahieu, E., Notholt, J., Rex, M., Bingen, C., Vanhellemont, F., Bourassa, A., Plane, J. M. C., Klocke, D., Carn, S. A., Clarisse, L., Trickl, T., Neely, R., James, A. D., Rieger, L., Wilson, J. C., and Meland, B., 2016: Stratospheric aerosol – Observations, processes, and impact on climate, *Rev. Geophys.*, **54**, 278–335, https://doi.org/10.1002/2015RG000511.

Krüger, K., Schäfler, A., Wirth, M., Weissmann, M., and Craig, G. C., 2022: Vertical structure of the lower-stratospheric moist bias in the ERA5 reanalysis and its connection to mixing processes, *Atmos. Chem. Phys.*, **22**, 15559–15577, https://doi.org/10.5194/acp-22-15559-2022.

Lawrence, Z. D., et al., 2022: Quantifying stratospheric biases and identifying their potential sources in subseasonal forecast systems, *Weather Clim. Dynam.*, **3**, 977–1001, https://doi.org/10.5194/wcd-3-977-2022.

Lim, E.-P., Hendon, H. H., Boschat, G., Hudson, D., Thompson, D. W. J., Dowdy, A. J., and Arblaster, J. M., Australian hot and dry extremes induced by weakenings of the stratospheric polar vortex, 2019: *Nat. Geosci.*, **12**, 896–901, https://doi.org/10.1038/s41561-019-0456-x.

Lim, E.-P., Hendon, H. H., Butler, A. H., Thompson, D. W. J., Lawrence, Z. D., Scaife, A. A., Shepherd, T. G., Polichtchouk, I., Nakamura, H., Kobayashi, C., Comer, R., Coy, L., Dowdy, A., Garreaud, R. D., Newman, P. A., and Wang, G., 2021: The 2019 Southern

Accepted for publication in *Bulletin of the American Meteorological Society.* DOI 10.1175/BAMS-D-24-0217.1.

Hemisphere stratospheric polar vortex weakening and its impacts, *Bull. Am. Meteorol. Soc.,* **102**, E1150–E1171, https://doi.org/10.1175/BAMS-D-20-0112.1.

McNally, A., C. Lessig, P. Lean, E. Boucher, M. Alexe, E. Pinnington, M. Chantry, S. Lang, C. Burrows, M. Chrust, F. Pinault, E. Villeneuve, N. Bormann, S. Healy, 2024: Data driven weather forecasts trained and initialised directly from observations, arXiv, https://doi.org/10.48550/arXiv.2407.15586.

Meul, S., Langematz, U., Kröger, P., Oberländer-Hayn, S., and Jöckel, P., 2018: Future changes in the stratosphere-to-troposphere ozone mass flux and the contribution from climate change and ozone recovery, *Atmos. Chem. Phys.*, **18**, 7721–7738, https://doi.org/10.5194/acp-18-7721-2018.

Monge-Sanz, B.M., Birner, T., Chabrillat, S., Diallo, M., Haenel, F., Konopka, P., Legras, B., Ploeger, F., Reddmann, T., Stiller, G., Wright, J.S., Abalos, M., Boenisch, H., Davis, S., Garny, H., Hitchcock, P., Miyazaki, K., Roscoe, H.K., Sato, K., Tao, M., Waugh, D., 2022a: Brewer-Dobson Circulation, Chapter 5 of the SPARC Reanalysis Intercomparison Project (S-RIP) Final Report, 165-219, https://aparc-climate.org/wp-content/uploads/2025/10/05_S-RIP_Report_Ch05.pdf.

Monge-Sanz, B. M., Bozzo, A., Byrne, N., Chipperfield, M. P., Diamantakis, M., Flemming, J., Gray, L. J., Hogan, R. J., Jones, L., Magnusson, L., Polichtchouk, I., Shepherd, T. G., Wedi, N., and Weisheimer, A., 2022b: A stratospheric prognostic ozone for seamless Earth system models: performance, impacts and future, *Atmos. Chem. Phys.*, **22**, 4277–4302, https://doi.org/10.5194/acp-22-4277-2022.

National Academies of Sciences, 2021: *Reflecting Sunlight: Recommendations for Solar Geoengineering Research and Research Governance*. Washington, DC: The National Academies Press. https://doi.org/10.17226/25762.

Neu, J. L., Flury, T., Manney, G. L., Santee, M. L., Livesey, N. J., and Worden, J., 2014: Tropospheric ozone variations governed by changes in stratospheric circulation, *Nat. Geosci.*, **7**, 340–344, https://doi.org/10.1038/ngeo2138.

Oh, J., Son, S.W., Choi, J., Lim, E. P., Garfinkel, C., Hendon, H., Kim, Y., and Kang, H. S., 2022: Impact of stratospheric ozone on the subseasonal prediction in the southern hemisphere spring, *Prog. Earth Planet. Sci.*, **9**, https://doi.org/10.1186/s40645-022-00485-4.

Accepted for publication in *Bulletin of the American Meteorological Society.* DOI 10.1175/BAMS-D-24-0217.1.

Orr, A., P. Bechtold, J. Scinocca, M. Ern, and M. Janiskova, 2010: Improved middle atmosphere climate and forecasts in the ECMWF model through a nonorographic gravity wave drag parameterization, *J. Clim.*, **23**, 5905-5926, https://doi.org/10.1175/2010JCLI3490.1.

Pierce, R. B., and T. D. A. Fairlie, 1993: Chaotic advection in the stratosphere: Implications for the dispersal of chemically perturbed air from the polar vortex, *J. Geophys. Res. Atmosphere*, **98**, 18589-18595, https://doi.org/10.1029/93JD01619.

Plane, J. M. C., Gumbel, J., Kalogerakis, K. S., Marsh, D. R., and von Savigny, C., 2023: Opinion: Recent developments and future directions in studying the mesosphere and lower thermosphere, *Atmos. Chem. Phys.*, **23**, 13255–13282, https://doi.org/10.5194/acp-23-13255-2023.

Plougonven, R., de la Cámara, A., Hertzog, A., Lott, F., 2020: How does knowledge of atmospheric gravity waves guide their parameterizations? *Q. J. R. Meteorol. Soc.*, **146**, 1529-1543, https://doi.org/10.1002/qj.3732.

Polichtchouk, I., Shepherd, T. G., and Byrne, N. J., 2018: Impact of parametrized nonorographic gravity wave drag on stratosphere-troposphere coupling in the Northern and Southern Hemispheres, *Geophys. Res. Lett.,* **45**, 8612–8618, https://doi.org/10.1029/2018GL078981.

Ray, E. et al., 2024: Age of air from in situ trace gas measurements: insights from a new technique, *Atmos. Chem. Phys.*, **24**, 12425–12445, https://doi.org/10.5194/acp-24-12425-2024.

Revell, L.E., Bannister, M.T., Brown, T.F.M. *et al.*, 2025: Near-future rocket launches could slow ozone recovery, *npj Clim. Atmos. Sci.*, **8**, 212, https://doi.org/10.1038/s41612-025-01098-6.

Rhode, S., Preusse, P., Ungermann, J., Polichtchouk, I., Sato, K., Watanabe, S., Ern, M., Nogai, K., Sinnhuber, B.-M., and Riese, M., 2024: Global-scale gravity wave analysis methodology for the ESA Earth Explorer 11 candidate CAIRT, *Atmos. Meas. Tech.*, **17**, 5785–5819, https://doi.org/10.5194/amt-17-5785-2024.

Richter, J. H., F. Sassi, and R. R. Garcia, 2010: Toward a physically based gravity wave source parameterization in a general circulation model, *J. Atmos. Sci.*, **67**, 136-156, https://doi.org/10.1175/2009JAS3112.1.

Accepted for publication in *Bulletin of the American Meteorological Society*. DOI 10.1175/BAMS-D-24-0217.1.

Ridley, D. A., et al., 2014: Total volcanic stratospheric aerosol optical depths and implications for global climate change, *Geophys. Res. Lett.*, **41**, 7763–7769, https://doi.org/10.1002/2014GL061541.

Riese, M., F. Friedl-Vallon, R. Spang, P. Preusse, C. Schiller, L. Hoffmann, P. Konopka, H. Oelhaf, Th. von Clarmann, M. Höpfner, 2005: GLObal limb Radiance Imager for the Atmosphere (GLORIA): Scientific objectives, *Advances in Space Research*, **36**, 989-995, ISSN 0273-1177, https://doi.org/10.1016/j.asr.2005.04.115.

Riese, M., Ploeger, F., Rap, A., Vogel, B., Konopka, P., Dameris, M., and Forster, P., 2012: Impact of uncertainties in atmospheric mixing on simulated UTLS composition and related radiative effects, *J. Geophys. Res. Atmospheres*, **117**, https://doi.org/10.1029/2012JD017751.

Riese, M., H. Oelhaf, P. Preusse, J. Blank, M. Ern, F. Friedl-Vallon, H. Fischer, T. Guggenmoser, M. Höpfner, P. Hoor, M. Kaufmann, J. Orphal, F. Plöger, R. Spang, O. Suminska-Ebersoldt, J. Ungermann, B. Vogel, and W. Woiwode, 2014: Gimballed Limb Observer for Radiance Imaging of the Atmosphere (GLORIA) scientific objectives, *Atmos. Meas. Tech.*, **7**, 1915-1928, https://doi.org/10.5194/amt-7-1915-2014.

Salawitch, R. J., J. B. Smith, H. Selkirk, K. Wargan, M. P. Chipperfield, R. Hossaini, P. F. Levelt, N. J. Livesey, L. A. McBride, L. F. Millán, E. Moyer, M. L. Santee, M. Schoeberl, S. Solomon, K. Stone, H. M. Worden, 2025: The imminent data desert: The future of stratospheric monitoring in a rapidly changing world, *Bulletin of the American Met. Soc.*, https://doi.org/10.1175/BAMS-D-23-0281.1.

Santer, B., Bonfils, C., Painter, J. et al., 2014: Volcanic contribution to decadal changes in tropospheric temperature, *Nature Geosci.*, **7**, 185–189, https://doi.org/10.1038/ngeo2098.

Saunders, L. N., et al., 2024: Age of air from ACE-FTS measurements of sulfur hexafluoride, https://doi.org/10.5194/egusphere-2024-2117.

Scaife, A. A., Baldwin, M. P., Butler, A. H., Charlton-Perez, A. J., Domeisen, D. I. V., Garfinkel, C. I., Hardiman, S. C., Haynes, P., Karpechko, A. Y., Lim, E.-P., Noguchi, S., Perlwitz, J., Polvani, L., Richter, J. H., Scinocca, J., Sigmond, M., Shepherd, T. G., Son, S.-W., and Thompson, D. W. J., 2022: Long-range prediction and the stratosphere, *Atmos. Chem. Phys.*, **22**, 2601–2623, https://doi.org/10.5194/acp-22-2601-2022.

Accepted for publication in *Bulletin of the American Meteorological Society.* DOI 10.1175/BAMS-D-24-0217.1.

Sellitto, P., Podglajen, A., Belhadji, R., et al., 2022: The unexpected radiative impact of the Hunga Tonga eruption of 15th January 2022, *Commun. Earth Environ.*, **3**, 288, https://doi.org/10.1038/s43247-022-00618-z.

Sellitto, P., Belhadji, R., Cuesta, J., Podglajen, A., and Legras, B., 2023: Radiative impacts of the Australian bushfires 2019–2020 – Part 2: Large-scale and in-vortex radiative heating, *Atmos. Chem. Phys.,* **23**, 15523–15535, https://doi.org/10.5194/acp-23-15523-2023.

Semane, N. and Bonavita, M., 2025: Reintroducing the analysis of humidity in the stratosphere, *ECMWF Newsletter*, **183**, 28-31, https://doi.org/10.21957/ns41h80kl3.

Sinnhuber, M. and Funke, B., 2020: Chapter 9 - Energetic electron precipitation into the atmosphere, in: The Dynamic Loss of Earth's Radiation Belts, edited by: Jaynes, A. N. and Usanova, M. E., Elsevier, 279–321, https://doi.org/10.1016/B978-0-12-813371-2.00009-3.

Solomon, S., Rosenlof, K. H., Portmann, R. W., Daniel, J. S., Davis, S. M., Sanford, T. J., and Plattner, G.-K., 2010: Contributions of stratospheric water vapor to decadal changes in the rate of global warming, *Science*, **327**, 1219–1223, https://doi.org/10.1126/science.1182488.

Solomon, S., Daniel, J. S., Neely, R. R., Vernier, J.-P., Dutton, E. G., and Thomason, L. W., 2011: The persistently variable "background" stratospheric aerosol layer and global climate change, *Science*, **333**, 866–870, https://doi.org/10.1126/science.1206027.

Solomon, S., Stone, K., Yu, P., Murphy, D. M., Kinnison, D., Ravishankara, A. R., and Wang, P., 2023: Chlorine activation and enhanced ozone depletion induced by wildfire aerosol, *Nature*, **615**, 259–264, https://doi.org/10.1038/s41586-022-05683-0.

Staten, P. W., Lu, J., Grise, K. M., Davis, S. M., and Birner, T., 2018: Re-examining tropical expansion, *Nat. Clim. Change*, **8**, 768–775, https://doi.org/10.1038/s41558-018-0246-2.

Stiller, G. P., von Clarmann, T., Höpfner, M., Glatthor, N., Grabowski, U., Kellmann, S., Kleinert, A., Linden, A., Milz, M., Reddmann, T., Steck, T., Fischer, H., Funke, B., Lopez-Puertas, M., and Engel, A., 2008: Global distribution of mean age stratospheric air from MIPAS SF_6 measurements, *Atmos. Chem. Phys.*, **8**, 677–695, https://doi.org/10.5194/acp-8-677-2008.

Accepted for publication in *Bulletin of the American Meteorological Society.* DOI 10.1175/BAMS-D-24-0217.1.

Stiller, G. P., von Clarmann, T., Haenel, F., Funke, B., Glatthor, N., Grabowski, U., Kellmann, S., Kiefer, M., Linden, A., Lossow, S., and López-Puertas, M., 2012: Observed temporal evolution of global mean age of stratospheric air for the 2002 to 2010 period, *Atmos. Chem. Phys.*, **12**, 3311–3331, https://doi.org/10.5194/acp-12-3311-2012.

Stone, K. A., Solomon, S., Kinnison, D. E., Pitts, M. C., Poole, L. R., Mills, M. J., Schmidt, A., Ryan R. Neely III, R. R., Ivy, D., Schwartz, M. J., Vernier, J.-V., Johnson, B. J., Tully, M. B., Klekociuk, A. R., König-Langlo, G., Hagiya, S., 2017: Observing the impact of Calbuco volcanic aerosols on South Polar ozone depletion in 2015, *J. Geophys. Res. Atmospheres,* **122**, 11,862–11,879. https://doi.org/10.1002/2017JD026987.

Thompson, D. W. J., Solomon, S., Kushner, P. J., England, M. H., Grise, K. M., and Karoly, D. J., 2011: Signatures of the Antarctic ozone hole in Southern Hemisphere surface climate change, *Nat. Geosci.*, **4**, 741–749, https://doi.org/10.1038/ngeo1296.

Tilmes, S. et al., 2024: Research criteria towards an interdisciplinary Stratospheric Aerosol Intervention assessment, Oxford Open Climate Change, 4(1), p. kgae010. https://doi.org/10.1093/oxfclm/kgae010.

Tirelli, C., Ceccherini, S., Del Bianco, S., Funke, B., Höpfner, M., Cortesi, U., and Raspollini, P., 2025: Extension of the Complete Data Fusion algorithm to tomographic retrieval products, *Atmos. Meas. Tech.,* **18**, 5619–5636, https://doi.org/10.5194/amt-18-5619-2025.

Voet, F., F. Ploeger, J. Laube, P. Preusse, P. Konopka, J.-U. Grooß, J. Ungermann, B.-M. Sinnhuber, M. Höpfner, B. Funke, G. Wetzel, S. Johansson, G. Stiller, E. Ray, and M. I. Hegglin, 2025: On the estimation of stratospheric age of air from correlations of multiple trace gases, *Atmos. Chem. Phys.,* **25**, 3541–3565, https://doi.org/10.5194/acp-25-3541-2025.

Woiwode, W., Dörnbrack, A., Polichtchouk, I., Johansson, S., Harvey, B., Höpfner, M., Ungermann, J., and Friedl-Vallon, F., 2020: Technical note: Lowermost-stratosphere moist bias in ECMWF IFS model diagnosed from airborne GLORIA observations during winter–spring 2016, *Atmos. Chem. Phys.*, **20**, 15379–15387, https://doi.org/10.5194/acp-20-15379-2020.

Accepted for publication in *Bulletin of the American Meteorological Society.* DOI 10.1175/BAMS-D-24-0217.1.

World Meteorological Organization (WMO), 2022: *Scientific Assessment of Ozone Depletion: 2022*, GAW Report No. 278, 509 pp.; WMO: Geneva.

Accepted for publication in *Bulletin of the American Meteorological Society.* DOI 10.1175/BAMS-D-24-0217.1.